Journal Name

ARTICLE

Structure and Reorientational Dynamics of 1-F-Adamantane

B. Ben Hassine,[a,b] Ph. Negrier,[a] M. Romanini,[c] M. Barrio,[c] R. Macovez,[c] A. Kallel,[b] D. Mondieig[a] and J. Ll. Tamarit[c,*]

The polymorphism and the dynamics of a simple rigid molecule (1-fluoro-adamantane) have been studied by means of x-ray powder diffraction and broadband dielectric spectroscopy. At temperatures below the melting, the molecule forms an orientationally disordered phase I with cubic-centered structure (Phase I, $Fm\bar{3}m$, Z=4). This phase possesses eight equilibrium positions for the fluorine atom, with equal occupancies factors of 1/8. A solid-solid phase transition to a low-temperature tetragonal phase (Phase II, $P\bar{4}2_1c$, Z=2) reduces the statistical disorder to only four possible equivalent sites for the fluorine atom, with fractional occupancies of 1/4. The dynamics has been rationalized under the constraints imposed by the space group of the crystal structure determined by powder X-ray diffraction. The dielectric spectroscopy study reveals that the statistical disorder in Phase II is dynamic in character and is associated with reorientational jumps along the two- and three-fold axes. In the dielectric loss spectra, the cooperative (α) relaxation exhibits a shoulder on the high-frequency side. This remarkable finding clearly reveals the existence of two intrinsic reorientational processes associated with the exchange of the F atom along the four sites. In addition to such "bimodal" relaxation, a secondary Johari-Goldstein relaxation is detected at lower temperatures.

Introduction

The dynamics of amorphous systems is one of the areas of greatest interest and challenging studies in the field of condensed matter physics.[1-4] The physics of disordered materials is particularly intriguing; in particular, a full understanding of the origin of the glass transition phenomenon in dynamically disordered systems (i.e., systems where the disorder is due to time-varying structural, orientational or molecular conformations) is still lacking.[5,6]

The dynamics of glass-forming liquids has been the subject of many experimental investigations, which have shown very diverse dynamic behavior.[4,6,7] Most of the research has been focused on "canonical" glasses, namely those obtained from the freezing (through a decrease in temperature or an increase in pressure) of both translational and orientational degrees of freedom.[8] The disorder in a condensed phase can however also be only partial, involving only a subset of all degrees of freedom. Partial disorder gives rise to different states of matter: liquid crystals are translationally disordered but orientationally ordered while, oppositely, plastic crystals are translationally ordered and orientationally disordered (OD).[9-13] For the latter materials, composed of globular shaped molecules, the molecular orientation is completely undetermined, as the molecules undergo free-rotor

motions. The class of solids with dynamic orientational disorder also comprises systems in which, at least in a certain temperature range, the thermal energy is not high enough to allow free rotations of the molecules, which rather perform reorientational jumps between well-defined, distinguishable orientations (compatible to the symmetry operations of the site in which they are located at the lattice). Decreasing the temperature slows down the reorientational jumps and can lead to the formation of a so-called "glassy crystal", the non-ergodic state of the OD phase. Nevertheless, there is also the possibility that a phase transition to a lower symmetry crystal occurs, which entails partial or complete reduction of the orientational disorder. A reduction of disorder through the transition to a low-temperature phase has been detailed recently for low-symmetry (monoclinic) phases of 2-adamantanone[14], $CBrCl_3$ and CBr_2Cl_2 [15,16], CCl_3-CF_2Cl[17] and $CHCl_2-CCl_2H$ [18,19].

The molecular dynamic processes in these systems have been found to display the same general features of those of canonical glasses. A universal feature of all glass formers is for example the existence of a collective dynamics whose slowing down marks the transition to the glassy state, i.e., the well-known α-(primary) relaxation process. A less cooperative dynamic relaxation, the so-called Johari-Goldstein (JG) process[20], is also commonly observed, at time scales faster than the primary relaxation. Such a process is generally considered a universal feature of glassy-like materials, but its origin is still a matter of debate[21]. Some models assign this feature to the existence of microscopic domains (islands of mobility) in which molecular mobility is higher due to a lower value of the local density[19], while some others ascribe it to small-angle reorientations displayed by all molecules alike.[22] In particular, for strong glasses according to the strong/fragile classification of Angell[23], some models claim the nonexistence of the JG-relaxation.[24] On the contrary, recent experimental results have shown the emergence of a glass-like α- and β-dynamic processes even in a quite ordered system, namely the low-temperature monoclinic phase of 2-

a. Univ. Bordeaux, LOMA, UMR 5798, F-33400 Talence, France, CNRS, LOMA, UMR 5798, F-33400 Talence, France.
b. Laboratoire des Matériaux Céramiques Composites et Polymères, Département Physique, Faculté des Sciences de Sfax, 3000 Sfax (Tunisie).
c. Grup de Caracterització de Materials, Department de Física, ETSEIB, Diagonal 647, Universitat Politècnica de Catalunya, 08028 Barcelona, Catalonia (Spain).
E-mail: josep.lluis.tamarit@upc.edu. +34 934016564

adamantanone, in which these processes were ascribed respectively to a strongly restricted collective reorientational motion and to local non-cooperative molecular motion, that is, to a genuine JG-relaxation. A clear β-relaxation was observed also in the low-temperature phases of $CBr_nCl_{(4-n)}$, n=0,1,2 compounds, a group of strong glasses with a well-defined disorder related to the occupancy of halogen sites. Such relaxation was ascribed to the presence of dynamic heterogeneities[15,16].

These unexpected results on very simple and "well-ordered" systems suggest that OD solids can be exploited as model playgrounds in which the physics behind the glass transition and the associated molecular relaxations can be more thoroughly investigated, with the hope of disentangling the origin of local, non-cooperative JG-relaxation. In order to pursue this goal, the present work discusses the dynamics of the low-temperature phase of a simple rigid molecule displaying statistical disorder. The material under scrutiny is 1-Fluoro-adamantane ($C_{10}H_{15}F$, hereinafter referred to as 1F-ada). Adamantane derivatives display a rich polymorphism that has stimulated a large number of experimental and theoretical investigations aimed at understanding the dynamics of the high-temperature OD phases and, to less extent, the low-temperature phases.[25-28]

1F-ada is a globular molecule with C_{3v} (3m) point-group symmetry, obtained from adamantane ($C_{10}H_{16}$) by replacing one of the hydrogen atoms attached to a three-coordinated (tertiary) carbon with a fluorine atom. Such substitution confers to the molecule a noticeable dipole moment (μ = 2.1 D).[29] Calorimetric (DSC) measurements revealed a solid-solid phase transition at 222 K, with an enthalpy and entropy of transition of 1.50 kJ. mol^{-1} and 6.77 J K^{-1}, respectively. The reported melting temperature is 525 K.[30] The solid phase of 1-F-ada between 525 K and 222 K is an OD crystal with cubic structure ($Fm\bar{3}m$ space group, hereafter Phase I),[31] whose structure and dynamics have been widely studied by numerous techniques, namely thermal analysis,[30] X-ray diffraction,[31] NMR,[32] single-crystal Raman scattering,[33] dielectric analysis[29], and incoherent quasi-elastic neutron scattering.[34] It was shown that the fluorine atom occupies 8 distinguishable equilibrium positions corresponding to so as many orientations along the [111] direction of the cubic lattice in such a way that the threefold molecular and crystal axes are coincident.[31] The relaxation observed with dielectric spectroscopy was assigned to jumps of the molecular dipole between neighboring [111] directions of the cubic lattice.[29] Incoherent quasielastic neutron scattering measurements showed the existence of two characteristic correlation times, corresponding one to the dipolar tumbling observed by dielectric spectroscopy and the other to uniaxial 120° rotations between three equilibrium positions around the molecular symmetry axis (along the C-F dipole direction).[34] Much less is known about the low temperature phase stable below 222 K (hereafter Phase II), on which we focus in this work.

Experimental details

1-Fluoro-adamantane was purchased from ABCR, with purity of 99% and used as received. To study the dynamics of the low-temperature phase II of 1F-ada, we have combined X-ray diffraction with broadband dielectric spectroscopy. Powder X-ray diffraction data were collected by means of a horizontally mounted INEL cylindrical position-sensitive detector (CPS 120). The detector, used in Debye-Scherrer geometry, is constituted by 4096 channels, providing an angular step of 0.029° (2θ) between 4° and 120°.

Monochromatic Cu $K_{\alpha 1}$ radiation (λ= 1.5406 Å) was selected with an asymmetric focusing incident-beam curved quartz monochromator. The samples were introduced into 0.5-mm-diameter Lindemann capillaries which rotate along their longitudinal axes during data collection to prevent the effects of the preferred orientations. The system is equipped with a liquid nitrogen 600 series Cryostream Cooler from Oxford Cryosystems with a temperature accuracy of 0.1 K and similar to fluctuations.

The relaxation times were measured by means of broadband dielectric spectroscopy conducted with a Novocontrol analyzer (10^{-2} to 10^7 Hz) and an HP4291 impedance analyzer (10^6 to 1.8×10^9 Hz), equipped with a Quatro temperature controller (±0.1 K) for measurements down to ca. 110 K and a closed-cycle helium cryostat for measurements down to ca. 60 K. The capacitor was prepared by pressing the 1F-ada powder between two stainless steel disks using a hydraulic press (120 kN).

To fit the dielectric spectra, a combination of a Havriliak-Negami (HN) function for the α relaxation and a Cole-Cole (CC) function for the α' and β relaxations was used. The general expression for the HN function is:[35]

$$\varepsilon_{NH}(f) = \varepsilon_\infty + \frac{\varepsilon_S - \varepsilon_\infty}{\left[1 + (i2\pi f\tau)^\alpha\right]^\beta}$$

Here ε_s and $\varepsilon_\square$ are the high-frequency and static low-frequency limits of the real permittivity and the exponents α and β are shape parameters with values between 0 and 1. τ_{HN} is a fitting parameter from which the characteristic time τ at which the dielectric loss of the primary relaxation process is maximum is obtained as:

$$\tau = \tau_{max} = \tau_{HN}\left(\sin\frac{\alpha\pi}{2+2\beta}\right)^{-1/\alpha}\left(\sin\frac{\alpha\beta\pi}{2+2\beta}\right)^{1/\alpha}$$

The equation of the Cole-Cole function can be expressed as:[36]

$$\varepsilon_{CC}(f) = \varepsilon_\infty + \frac{\varepsilon_S - \varepsilon_\infty}{1 + (i2\pi f\tau_{CC})^\alpha}$$

In this case the characteristic time τ corresponds to the fitting parameter τ_{CC}.

Results and discussion

The lattice and possible space groups of phases I and II were determined at 295 and 100 K, respectively, by means of X-Cell software, available in the module Powder Indexing of Materials Studio,[37] according to a reasonable density and compatibility between the volume change at the II-I transition. Pawley refinement,[38] which minimizes the weighted R-factor, R_{wp}, describing the agreement between the experimental and the simulated patterns, helps to confirm the indexing result and the systematic absences for the space group assessment. In order to determine the structure of the two crystalline phases we have built up the molecule of 1F-ada using the parameters defining the adamantane molecule $C_{10}H_{16}$,[39] replacing one hydrogen atom in the molecule of adamantane by a fluorine one. The carbon atom C_1 and the fluorine atom F are placed on the diagonal of the cube and the carbon atom C_2 is placed on a cube axis. The distance between the atoms and the centre of mass (origin of the cube) "O" has the

following value: OF_1 = 2.90 Å, OC_1 = 1.530 Å, OC_2 = 1.765 Å. Parameters defining the rigid molecule are: C—H 1.529 Å, C—F 1.370 Å and C—C 1.970 Å. The final Rietveld refinement,[40] position and orientation of the molecule, within the rigid-body constraint, with a single overall isotropic displacement parameter and preferred orientation by using the Rietveld-Toraya function[41] were refined. The final refined patterns are depicted in Figures 1a and 1b for phases I and II, respectively, together with the experimental and refined pattern difference. The Rietveld refinement converged to a final R_{wp} value of 6.19% and 4.07% for phases I and II, respectively.

The refined structure of the high-temperature phase I of 1F-ada is face-centred cubic (Fm$\bar{3}$m), with four molecules per unit cell and a = 9.5522(4) Å at 295 K (see Figures 2a and 2b). This phase possesses eight equilibrium positions for the fluorine atom, with equal fractional occupancy of 0.125. These results match those of the earlier study by means of single crystal diffraction mentioned in the Introduction.[31]
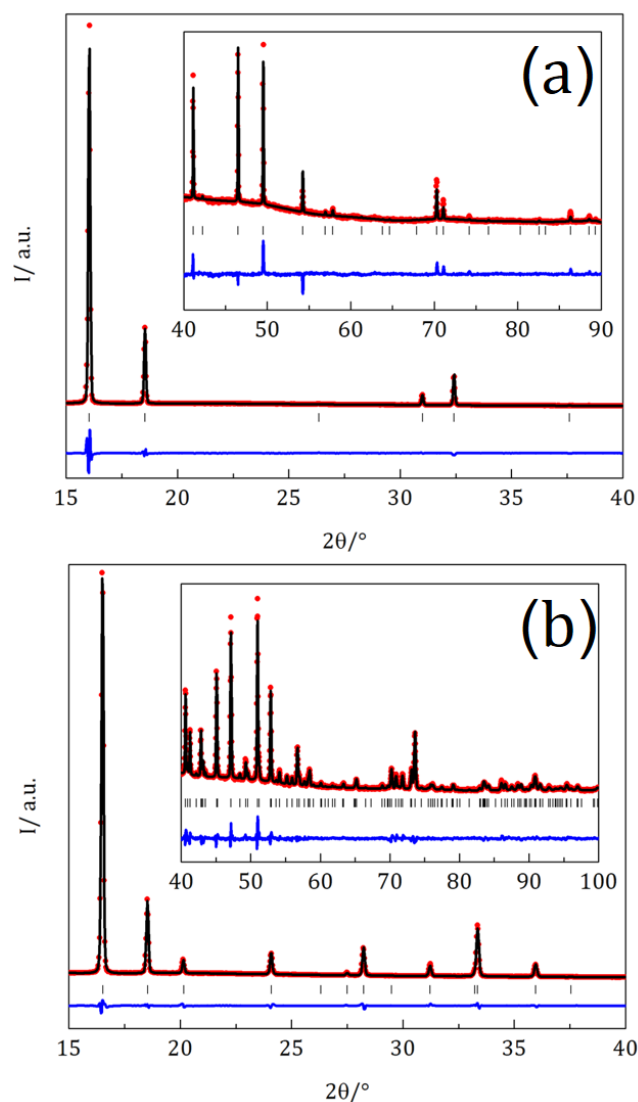
When cooling from phase I to phase II previous results indicated that the single crystal breaks and thus powder diffraction is the only way to determine the structure of the low-temperature phase II. We determined the lattice symmetry of phase II to be tetragonal, space group P$\bar{4}$2$_1$c, with two molecules per unit cell, Z= 2, one molecule per asymmetric unit, Z'=1, and lattice parameters a = b = 6.7776(3) Å, and c = 8.8235(5) Å at 100 K. The most striking feature of the structure of phase II is the existence of statistical intrinsic disorder concerning the site occupancy of the fluorine atom. As can be seen in the Figures 2c and 2d, four possible sites are occupied by the fluorine atom with temperature-independent fractional occupancies of 0.25.

In Figure 2c, we present four cells along the **c** axis of the structure of this tetragonal phase in order to highlight the resemblance between the stacking of both tetragonal and cubic structures. It can be noticed that both structures have a very close stacking with a slight difference: a rotation of 6.65° of the molecule along the **c** axis in phase II with respect to phase I. As a consequence of the four different molecular orientations in the low-temperature phase II, large-angle rotations around a twofold and a threefold axes (see insets in Figure 5) which would exist for a molecule devoid of the fluorine atom, appear. These rotations result in an effective time-average fluctuation of the molecular dipole which causes a contribution to the dielectric susceptibility.

The structural solutions for phases I and II determined respectively at 295 and 100 K were also verified for other temperatures. To do so, X-ray powder diffraction measurements were conducted from 90 to 360 K. Diffraction patterns were collected every 20 K and every 5 K close to the II-I transition. The variation as a function of temperature of the lattice parameters a_I for phase I, and $a' = a_{II}\sqrt{2}$ and c_{II} for phase II, are drawn in Figure 3a.
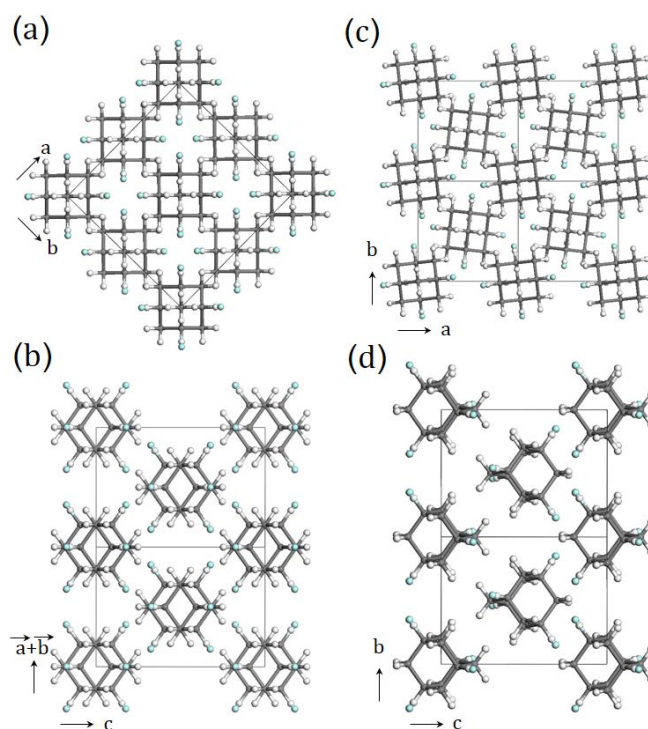

Fig. 1 Experimental (red circles) and Rietveld refined (black line) diffraction patterns along with the difference profile (blue line) and Bragg reflections (vertical sticks) : a) of the cubic Fm$\bar{3}$m space group phase I at 295 K of 1-Fluoro-adamantane and b) of the tetragonal P$\bar{4}$2$_1$c space group phase II at 100 K. The insets show the high-angle portion of each pattern (scaled to enhance their visibility): a) between 40° and 90°, magnified 45 times and b) between 40° and 100°, magnified 25 times.

Fig. 2 Crystal structures of 1-Fluoro-adamantane: phase I at 295 K (a) *along c* and (b) *along a+b*; phase II at 100 K (c) *along c* and (d) *along a*. Blue atoms correspond to the Fluorine atom within their eight sites of fractional occupancies 0.125 for cubic phase (I) and four sites of fractional occupancies 0.25 for the tetragonal phase (II).

The variation of the volume per molecule, V/Z, for both phases I and II is displayed in Figure 3b. The discontinuity across the II-I transition confirms its first-order character.

While diffraction techniques cannot provide information about the dynamics of the dipole reorientation, they highlight the disorder and quantify unequivocally the possible molecular orientations within the commensurate long-range lattice. It is important to note that, since the fractional occupancies of the four orientational sites have been shown to be independent of temperature, this means that a sort of local symmetry is preserved. This can only occurs if correlations exist among motions of different molecules.
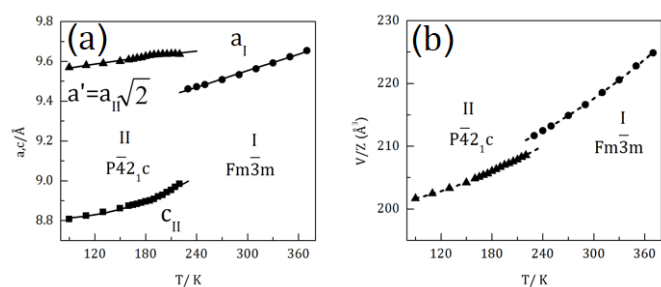

Fig. 3 Variation with temperature of the unit cell parameters (a'= a_{II} $\sqrt{2}$, c_{II}, a_{I}) of 1-Fluoro-adamantane (▲ and ■ phase II; ● ...

comparison, unit cell parameter a_{II} has been multiplied by $\sqrt{2}$) (left panel) and of the volume per molecule (V/Z) for the two solid phases I and II (Z_I=4 and Z_{II} =2, respectively) (right panel).

In order to confirm the dynamic character of the occupational disorder of the F atom within the tetragonal phase II and to fully characterize such dynamics, a dielectric spectroscopy study was undertaken. Molecular motions are readily detected with this technique owing to the dipole moment of the 1F-ada molecule (μ = 2.1 D). Figure 4 shows several representative examples of dielectric loss spectra of 1F-ada from 216 K down to 64 K. The most prominent feature is the existence of a clear relaxation peak (α-relaxation) whose maximum continuously shifts to lower frequencies with decreasing temperature, thus revealing the freezing of the collective molecular dynamics. The frequency of maximum loss is close to the early dielectric studies of Amoureux et al.[29] In that work the dielectric loss spectra had only very sparse points and were fitted with two different types of functions, namely a Cole-Cole for T>130 K and a Cole-Davison for T<130 K. Our data clearly show the existence, in addition to the main peak (α relaxation), of an excess wing (hereinafter called α' relaxation) appearing as a shoulder to the main peak, as well as of a β-relaxation appearing in the low-temperature spectra (below 88 K).

The fitting of the most prominent feature with only one Havriliak-Negami function did not reproduce the spectra, precisely due to the presence of the shoulder. As shown in Figure 4, two relaxation processes are needed for describing the experimental data in this frequency range. Accordingly, spectra were fitted using a Havriliak-Negami function for the main α relaxation and a Cole-Cole function for the shoulder, the α' relaxation (a fit of the α' relaxation with the HN function always resulted in β_{HN} very close to 1). Fits are displayed with continuous lines in figure 4.

A representative example of both contributions to the fit is shown for the spectrum at 128 K by dashed lines. The exponents resulting from the HN fits lie in the rannges $0.71 < \alpha_{HN} < 1$ and $0.85 < \beta_{HN} < 1$ for the α-relaxation, and $0.61 < \alpha_{CC} < 1$ for the α' relaxation. According to the Alvarez-Alegria-Colmenero equation[42], the stretching exponent β^{KWW} describing the spectral relaxation

function in the time domain can be calculated as $\beta^{KWW} = (\alpha_{HN} \cdot \beta_{HN})^{\frac{1}{1.23}}$. This exponent changes from values around 1 at high-temperature, i.e. close to the II to I transition, to values of ca. 0.67 at temperatures close to the glass transition temperature (92.3 K) for both α and α' relaxations. This experimental fact clearly evidences that orientational correlations between nearest neighbors ascribed to many-body molecular motions increase with decreasing temperature. It is worth mentioning that values close to 1 for the stretching exponent β^{KWW} were also found in the high-temperature phase I, indicating that the average packing does not change noticeably across the I to II transition.[29]
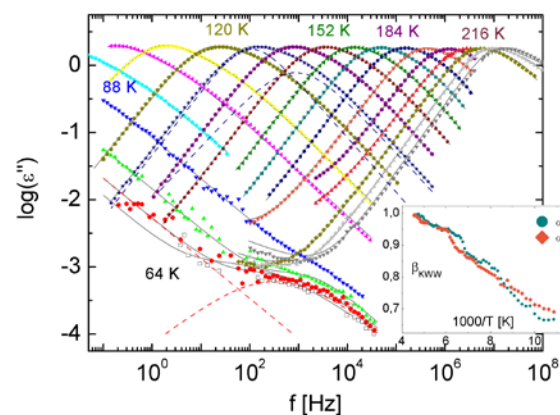

Fig. 4 Dielectric loss spectra of 1F-ada from 216 to 64 K, every 8 K. Symbols are experimental points, while the solid lines represent the fits of the spectra as the sum of two components. For the spectrum at 128 K dashed lines indicate the two components (HN and CC) used for the fit, while for the spectrum at 64 K the linear component and the CC functions are depicted with red dashed lines. Inset: stretching exponent β^{KWW} as a function of the reciprocal of temperature.

The relaxation times obtained for the both α and α' relaxations are collected in Figure 5 as a function of the reciprocal of temperature together with previously published relaxation times.[29,34] Both α and α' processes follow an Arrhenius temperature behaviour, with activation energies of 3709±10 K (30.84 ±0.08 kJ mol^{-1}) and 3517±11 K (29.24 ±0.10) kJ mol^{-1}) and pre-exponential factors of $\tau_o(\alpha)$=2.9·10^{-15} s and $\tau_o(\alpha')$=0.17·10^{-15} s, respectively. Both activation energies are significantly higher than that characterizing the high-temperature phase I, determined to be 24.4±0.08 kJ mol^{-1} from dielectric spectroscopy[29] or 19.0 kJ mol^{-1} from quasielastic neutron scattering[34]. The difference is likely due to the higher steric hindrance in the low-temperature phase. According to the α-relaxation values, the glass transition is determined to be at $T_g(\tau_\alpha$=100 s)=92.3 K, in agreement with previous published values.[29] It is worth noting that the relaxation times from Amoureux et al.[29] who reported only one relaxation process, match quite well with values of the present work for the α relaxation at high-temperature, but diverge at low temperature (see Figure 4) in such a way that values are much closer to those of the α' relaxation as temperature decreases. Due to such a difference the activation energy was reported as 3502 K, which is instead close to the value for the faster α' relaxation.

The experimental "bimodal" (α, α') relaxation scheme can be rationalized based on the structural disorder concerning the statistical site occupancy of the fluorine atom. Such a disorder, identified in our x-ray diffraction analysis, is related to the existence

of a twofold and a threefold symmetry axes around which the 1-F-ada molecule can perform reorientational motions (see insets in Figure 5), which are accompanied by large-angle rotations of the molecular dipole contributing to the dielectric susceptibility. Probably, as it has been demonstrated for the high-temperature phase I,[34] rotations around the C-F molecular symmetry axis are also present, but they leave invariant the dipole moment and thus they cannot be observed by dielectric spectroscopy. Because rotation of only one single molecule around the twofold axis cannot occur due to steric hindrance, the observed disorder must result from a highly cooperative motion, which is energetically expensive. Based on this, we ascribe the primary α-relaxation to twofold rotations, whereas the faster α' relaxation, that also has lower activation energy, is ascribed to rotations around the threefold axis, as these are characterized by lower steric hindrance in the structure of Phase II. Because 1F-ada is a rigid molecule,[43,44] it cannot exhibit any "internal" relaxation associated with intramolecular dipole moment changes within the analyzed frequency range. This means that the fast β relaxation (whose characteristic relaxation time is plotted in Figure 5) should be ascribed to a Johari-Goldstein (JG) relaxation.

This process involves only local environments in which molecules perform small-angle thermally activated reorientational motions according to an homogenous interpretation[22] or motions due to the existence of "islands of mobility" due to the structural inhomogeneities[20,45]. Several reasons plead for this argument. First, there are no other possible whole molecular rotations along different symmetry axes compatible with the space group symmetry of the tetragonal phase, in addition to those giving rise to the α- and α'-relaxations. Second, the number of molecules in the asymmetric unit is just one, so the existence of heterogeneous dynamics appearing as a consequence of different relaxations from different molecules is not possible.[15,16]
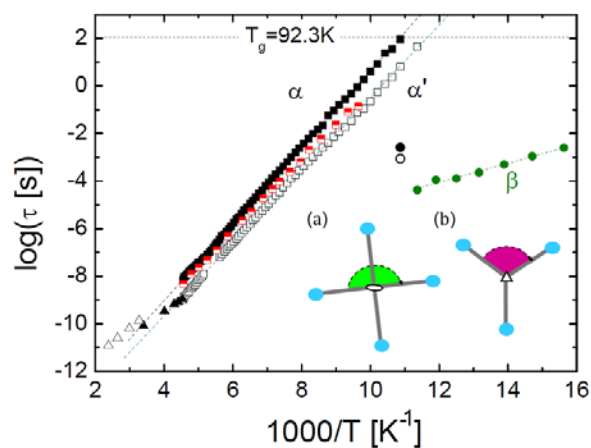

Fig.5 Relaxation times as a function of reciprocal of temperature for the different relaxation processes. Phase II: α (full black squares), α' (empty black squares) and β (full green circles) from this work. Full-empty red squares are relaxation times obtained from Amoureux et al.[29]. Empty and full black circles are the predicted β relaxation according to the Coupling Model.[21] Phase I: α-relaxation obtained from quasielastic neutron scattering in Ref. 34 (empty black triangles) and from dielectric spectroscopy in Ref. 29 (full black triangles). Dashed lines represent the Arrhenius fits. Insets are the projection of the F atom representing the large-angle rotations around the twofold axis (a) and the threefold axis (b) of the tetragonal structure (space group P $\bar{4}$ 2₁c).

The JG character of the relaxation may in some cases be checked by comparing the experimental data with the predictions of the so-

called coupling model (CM)[21], according to which the JG relaxation process should exhibit very similar relaxation time as the precursor motion of the main α relaxation. According to the CM, the β_{JG} and the α-relaxation times should be roughly linked through the equation:

$$Log(\tau_{JG})=(1-\beta^{KWW})Log(t_c)+ \beta^{KWW}Log(\tau_\alpha)$$

where t_c is a cross-over time of the order of 2 ps.

The coupling model is expected to hold at high temperature, namely above the glass transition. Unfortunately, the strength of the β_{JG} relaxation is quite small (see Figure 4), so that it is difficult to perform a reliable fit at temperatures higher than the glass transition temperature T_g. We can still compare the prediction of the coupling model with the experimental data close to the glass transition temperature. As visible in Figure 5, the calculated values for the JG relaxation times according to the CM employing ether the the α or α' fit parameters are not far away from the experimental β_{JG} relaxation times, although a discrepancy is observed. Similar deviations at sub-T_g temperatures have been found in structural glasses and attributed to the non-equilibrium state of the system[46,47].

The β_{JG} relaxation in Phase II follows, as it is usually found, an Arrhenius law below the glass transition temperature with activation energy of 919 K (7.64±0.38 kJ·mol⁻¹) and pre-exponential factor of $\tau_o(\beta)=1.4 \cdot 10^{-9}$ s (see Figure 5). The situation at T>T_g is less clear because β_{JG} relaxation is generally swallowed by the nearby α-process. Moreover, in the present case, the existence of a shoulder (α' relaxation) adds an additional difficulty.

Conclusions

The results here reported on provide clear evidence that universal properties pertaining to the glass behavior also apply to solid state disordered matter, as we show for the particular case of 1-Fluoro-adamantane. We demonstrate that the low-temperature Phase II of 1-Fluoradamantane (space group P $\bar{4}$ 2₁c) displays an intrinsic statistical disorder concerning the site occupancy of the fluorine atom. We further show that such statistical disorder is dynamic in character, and is in fact the consequence of the existence of large-angle rotations around a twofold and a threefold axes, which would exist for a molecule devoid of the fluorine atom. Such rotations give rise to a bimodal primary relaxation, namely to a more prominent α relaxation, visible as a loss peak in the imaginary dielectric susceptibility, and to an α' relaxation visible as a shoulder to the latter peak. Moreover, a secondary β-relaxation, identified as a Johari-Goldstein relaxation (due to the rigid character of the molecule, no intramolecular relaxations exist), has been found at temperatures below the glass transition. Both α and α' relaxations display an Arrhenius behavior, thus indicating a strong character of this glasslike system according to Angell's classification, in spite of the low value of the stretching β^{KWW} parameter of both relaxations close to the glass transition.

To the best of our knowledge, this is the first time that two distinct primary relaxations are observed for separate rotational degrees of freedom of the same rigid molecule. Such a feature can only be shared by OD systems where the intermolecular interactions are strongly anisotropic and not by other types of glass formers such as supercooled liquids or plastic crystals, which display isotropic rotations. Our work demonstrates orientationally disordered phases as a class of systems with richer and more varied relaxation dynamics than "conventional" glass formers. Considering that many rigid molecular structural glass-formers are prone to crystallization

and not amenable for study, orientationally disordered solids displaying the universal features of glasses are thus ideal systems in which structure and dynamics should allow a deeper understanding of the underlying physics. In particular, these systems are a unique opportunity to elucidate the isomorph invariance of the structure and dynamics theory recently generalized for classical crystals.[48,49]

Acknowledgements

References

1 P. G. Debenedetti and F. H. Stillinger, *Nature (London)*, 2001, **410**, 259.

2 C. A. Angell, K. L. Ngai, G. B. McKenna, P. F. McMillan, and S. W. Martin, *J. Appl. Phys.,* 2000, **88**, 3113.

3 K. L. Ngai, *J. Non-Cryst. Solids*, 2007 ,**353**, 709-718.

4 P. Lunkenheimer, U. Schneider, R. Brand, and A. Loidl, *Contemp. Phys.,* 2000, **41**, 15.

5 P. W. Anderson, *Science*, 1995, **267**, 1615.

6 M. D. Ediger, C. A. Angell, and S. R. Nagel, *J. Phys. Chem.*, 1996, **100**, 13200-13212.

7 S. N. Tripathy, Z. Wojnarowska, J. Knapik, H. Shirota, R. Biswas, M. Paluch, *J. Chem. Phys.*, 2015, **142**, 184504.

8 M. Jiménez-Ruiz, A. Criado, F. J. Bermejo, G. J. Cuello, F. R. Trouw, R. Fernandez-Perea, H. Löwen, C. Cabrillo, and H. E. Fischer, *Phys. Rev. Lett.,* 1999, **83**, 2757.

9 H. M. Huffman, S. S. Todd, and G. D. Oliver, *J. Am. Chem. Soc.,* 1949, **71**, 584.

10 K. Adachi, H. Suga, and S. Seki, *Bull. Chem. Soc. Jpn.,* 1972, **45**, 1960.

11 M. Sorai and S. Seki, *Mol. Cryst. Liq. Cryst.,* 1973, **23**, 299.

12 H. Suga and S. Seki, *J. Non-Cryst. Solids,* 1974*,* **16**, 171-194.

13 C. A. Angell, L. E. Busse, E. I. Cooper, R. K. Kadiyala, A. Dworkin, M. Ghelfenstein, H. Szwarc, and A. Vassal, *J. Chim. Phys. Phys.-Chim. Biol.,* 1985, **82**, 267.

14 M. Romanini, Ph. Negrier, J. Ll. Tamarit, S. Capaccioli, M. Barrio, L. C. Pardo, and D. Mondieig, *Phys. Rev. B*, 2012, **85**, 134201.

15 M. Zuriaga, L. C. Pardo, P. Lunkenheimer, J. Ll. Tamarit, N. Veglio, M. Barrio, F. J. Bermejo, and A. Loidl, *Phys. Rev. Lett.*, 2009, **103**, 075701.

16 M. J. Zuriaga, S. C. Perez, L. C. Pardo and J. Ll. Tamarit, *J. Chem. Phys.,* 2012, **137**, 054506.

17 Ph. Negrier, M. Barrio, J. Ll. Tamarit, L. C. Pardo, and D. Mondieig, *Cryst. Growth Des.*, 2012, **12**, 1513–1519.

18 S. C. Pérez, M. Zuriaga, P. Serra, A. Wolfenson, Ph. Negrier and J. Ll. Tamarit, *J. Chem. Phys.,* 2015, **143**, 134502.

19 Ph. Negrier, M. Barrio, J. Ll. Tamarit, D. Mondieig, M. Zuriaga, S.C. Pérez, *Cryst. Growth Des.,* 2013*,* **13**, 2143-2148.

20 G. P. Johari and M. Goldstein, *J. Chem. Phys.*, 1970, **53**, 2372.

21 K. L. Ngai, Relaxation and Diffusion in Complex systems, *Springer Science & Business Media*, *New York*, 2011.

22 F. H. Stillinger, *Science*, 1995, **267**, 1935-1939.

23 C.A. Angell, *Science*, 1995, **267**, 1924-1935.

24 H. Tanaka, *Phys. Rev. E*, 2004, **69**, 021502.

25 Y. Huang, D. F. R. Gilson, I. S. Butler, and F. Morin, *J. Phys. Chem.,* 1991, **95**, 2151-2156.

26 N. Arul Murugan, R. S. Rao, S. Yashonath, S. Ramasesha, and B. K. Godwal, *J. Phys. Chem. B*, 2005, **109**, 17296-17303.

27 J. P. Amoureux, M. Bee, and J. C. Damien, *Acta Cryst. B*, 1980, **36**, 2633-2636.

28 N. Arul Murugan and S. Yashonath, *J. Phys. Chem. B*, 2005, **109**, 2014-2020.

29 J. P. Amoureux, M. Castelain, M. Bee, M. D. Benadda, and M. More, *Mol. Phys*., 1985, **55**, 241-251.

30 T. Clarck, T. Mc. O. Kknox, H. Mackle, and M. A. Mckervey, *J. Chem. Soc. Faraday Trans. 1*, 1977, **73**, 1224.

31 J. P. Amoureux, M. Bee, and J. L. Sauvajol, *Acta Cryst. Sect. B*, 1982, **38**, 1984-1989.

32 J. P. Amoureux, R. Decressain, and M. Castelain, Edited by J. Lascombe. *Elsevier Science Publishers B.V., Amsterdam.,* 1987, **46**, 559.

33 Y. Guinet, J. L. Sauvajol, and M. Muller, *Mol. Phys.,* 1988, **65**, 723-738.

34 M. Bee and J. P. Amoureux, *Mol. Phys.,* 1983, **50**, 585.

35 S. Havriliak and S. Negami, *J. Polym. Sci.-Pt. C*, 1966, **16**, 99–117; S. Havriliak and S. Negami, *Polymer*, 1967, **8**, 161–210.

36 K. S. Cole and R. H. Cole, *J. Chem. Phys.,* 1941, **9**, 341.

37 MS Modeling (Materials Studio), version 5.5. http://accelrys.com/products/collaborative-science/biovia-materials-studio.

38 G. S. Pawley, *J. Appl. Crystallogr.,* 1981, **14**, 357–361.

39 J. P. Amoureux, and M. Foulon, *Acta Cryst. B*, 1987, **43**, 470-479.

40 H. M. Rietveld, *J. Appl. Crystallogr.,* 1969, **2**, 65.

41 H. Toraya, F. Marumo, *J. Mineral.,* 1981, **10**, 211.

42 F. Alvarez, A. Alegría, and J. Colmenero, *Phys. Rev. B*, 1991, **44**, 7306.

43 N. T. Kawai, D. F. R. Gilson and I. S. Butler, *J. Chem.,* 1991, **69**, 1758.

44 A.C. Legon, J. Tizard and Z. Kisiel, *J. Molec. Struct.,* 2002, **612**, 83-91.

45 G. P. Johari, *J. Non-Cryst. Solids*, 2002, **317**, 307–310.

46 P. Lunkenheimer, L. C. Pardo, M. Köhler, A. Loidl, *Phys. Rev. E*, 2008, **77**, 031506.

47 D. Prevosto, S. Capaccioli, M. Lucchesi, P. A. Rolla, K.L. Ngai, *J. Chem. Phys.,* 2004, **120**, 4808.

48 D. E. Albrechtsen, A. E. Olsen, U. R. Pedersen, T. B. Schroder and J. C. Dyre, *Phys. Rev. B*, 2014, **90**, 094106.

49 J. C. Dyre, *J. Phys. Chem. B*, 2014, **118**, 10007-10024.